

*Short Communication*

## **On the Proportion of Pb and Pt in Carbon-Supported Electrocatalysts**

*G.S. Buzzo<sup>1</sup>, M.J.B. Orlandi<sup>1</sup>, E. Teixeira-Neto<sup>2</sup> and H.B. Suffredini<sup>1,\*</sup>*

<sup>1</sup> Universidade Federal do ABC, Centro de Ciências Naturais e Humanas, Rua Santa Adélia 166, Bairro Bangu, Santo André, SP, Brazil.

<sup>2</sup> Universidade de São Paulo, Departamento de Química Fundamental, Av. Prof. Lineu Prestes, 748, Butantã, 05508-000 - São Paulo - SP.

\*E-mail: [hugo.suffredini@ufabc.edu.br](mailto:hugo.suffredini@ufabc.edu.br)

*Received:* 12 July 2011 / *Accepted:* 15 August 2011 / *Published:* 1 September 2011

This short report discusses the effects of different proportions of Pb and Pt in several anodes that were synthesised at a fixed catalyst load of 10 % with respect to the carbon powder support. In these studies, formic acid was used as a model molecule to determine the relationship between the proportions of metals and electrocatalytic effects. X-ray diffraction (XRD) showed that the metal distribution was composed of separated crystallographic phases, and the formation of Pt-Pb alloys was not observed. Transmission electron microscopy (TEM) images demonstrated that the catalysts were heterogeneously dispersed onto the carbon powder support and that the quantity of lead was directly related to the size of the particles distributed onto the carbon support. Finally, electrochemical tests indicated that the 25% Pt - 75% PbO<sub>x</sub>-based catalyst performed best in the comparative study.

**Keywords:** Formic Acid Oxidation; Electrochemistry; TEM; Lead-based catalysts; DRX

### **1. INTRODUCTION**

Due to growing energy needs and the necessity of clean and efficient energy, several groups around the world are conducting research on fuel cells. In this context, direct formic acid fuel cells (DFAFCs) have received a great deal of attention in recent years because they present interesting results when compared with fuel cells that operate with methanol and ethanol as fuel [1,2].

Palladium is the reference material used to promote the oxidation of formic acid in these fuel cells [3,4]; additionally, some bi-metallic materials, including Pd-Pb alloys [5], have shown promising results in the oxidation of formic acid. Other materials based on Pt, Pb and Bi [6] have also been shown to perform well and have high tolerance to carbon monoxide (CO) poisoning during the oxidation of formic acid. In a recent publication, our research group discussed the properties of some

Pd, Pt and Pb-based catalysts. The main conclusion of this work was that the Pd-Pt-PbO<sub>x</sub>/C catalyst demonstrated a superior performance due to the synergistic effect of lead in the anode [7].

Concerning the oxidation compartment, the material used for the anode in fuel cells can be synthesised by a variety of methods that result in different structures, such as intermetallic phases [8] and core-shell structures [9]. In this context, the sol-gel method is a simple and effective technique to promote the synthesis of electrocatalysts [10,13].

Further discussion is focused on the quantities of catalysts deposited on carbon powder, which is commonly used as a support for fuel cell catalysts. Lin et al. [14] studied the effect of cerium content in Pt and Ce-based catalysts and concluded that a cerium content of 20 % in the catalyst was necessary to promote CO oxidation. In another study, Li et al. [15] examined the metal composition of Pt-Fe/C catalysts that were synthesised by the ethylene-glycol route to promote methanol oxidation. The authors concluded that a Pt:Fe ratio of 1.2:1 was optimal. Camara et al. [16] determined that the ethanol oxidation reaction was heavily dependent on the metallic composition, and the optimal atomic proportion of metals was determined to be Pt:Ru in a ratio of 60:40.

A great deal of research has focused on decreasing the use of noble metals due to the high cost of these metals, such as platinum and palladium [17]; specifically, several studies have examined ways to reduce Pt content in catalysts [18]. For instance, Billy et al. [19] studied ultra-low loadings of Pt in the cathode and anode and demonstrated that it is possible to use Pt loadings as low as 35 µg Pt cm<sup>-2</sup>, which is very low compared to state-of-the-art catalysts.

In this work, physical characterisations for several materials were conducted using XRD in an effort to qualify the structure of each material. Additionally, transmission electron microscopy (TEM) was used to observe the morphology of the catalysts. An extensive work concerning the structural properties of Pt and Pb-based catalysts was recently published by our group [20] that demonstrated the decisive role of lead in the electrocatalysis of formaldehyde.

The present work examines the effect of Pt and Pb composition in carbon-supported electrocatalysts with a fixed catalyst load of 10% with respect to the quantity of support on the oxidation of formic acid in sulphuric acid media.

## 2. EXPERIMENTAL

### 2.1. Working electrode preparation

An adapted sol-gel method was used as the synthesis route. Similar protocols have been described in previous publications from our group [10,21]. In short, acetylacetones of Pt and Pb were prepared in a mixture of ethanol and acetic acid (3:2, v/v) at appropriate concentrations and added to 0.2 g of carbon powder (Vulcan® XC72R) to achieve a catalyst nominal load of 10% (w/w with respect to the carbon powder). Several proportions of Pt and Pb were tested and varied from 10% Pt - 90% Pb to 90% Pt - 10% Pb. All modified powders were treated for 1 hour at a temperature of 400°C under a nitrogen atmosphere.

A fixed quantity of 1 mL of water and 0.04 mL of a 5% Nafion® solution (5% in aliphatic alcohols) were added to a mixture containing 0.008 g of each modified powder. The mixtures were placed in an ultrasonic bath for about 5 minutes to produce “black inks”. Next, 5  $\mu\text{L}$  of the ink was transferred to a glassy carbon electrode (geometric area of 0.031  $\text{cm}^2$ ) that had been previously polished with alumina, and the samples were washed with isopropyl alcohol and dried using an infrared light.

## 2.2. Reagents, Apparatus and Solutions.

Similar protocols have been described in previous publications [10, 20]. XRD data were recorded in a Rigaku diffractometer (Miniflex model) using Cu K $\alpha$  as the radiation source (1.5406  $\text{\AA}$ , 30 kV and 15 mA). For each measurement, 30 mg of the powdered samples was placed in a glass sample holder and compressed with a glass slide to obtain a uniform distribution. The  $2\theta$  Bragg angles were scanned over a range of 10-100° at a rate of 2° per minute with a 0.02° angular resolution. The distributions of the catalyst deposited on the carbon were investigated by TEM with a JEOL JEM 2100 microscope operating at 200 kV.

All electrochemical measurements were conducted in AUTOLAB PGSTAT 100 potentiostat/galvanostat equipment. The electrochemical experiments were performed in a Pyrex® glass cell equipped with three electrodes. The supporting electrolyte was a 0.5 mol  $\text{L}^{-1}$   $\text{H}_2\text{SO}_4$  solution (Merck) + 1.0 mol  $\text{L}^{-1}$  of formic acid (Synth). The reference electrode was a hydrogen electrode in the same solution (HESS), and the auxiliary electrode was a 2  $\text{cm}^2$  Pt foil.

## 3. RESULTS AND DISCUSSION

### 3.1. Physical characterisation

#### 3.2.1. X-ray diffraction

X-ray diffraction experiments were carried out under the same conditions with the goal of characterising the differences among the catalysts. All results are presented in Fig. 1 to qualitatively identify the phases present in each material. The relative intensities (counts per second) are presented in arbitrary units.

Fig. 1 shows that a higher Pt content is related to a higher Pt signal, which corroborates qualitatively with the expected proportion of metals. The five main reflections from the planes (111, 200, 220, 311 and 222) are seen in the XRD patterns of each material. The exact matching of these Pt reflections evidences the existence of separated crystallites of pure Pt in these catalysts. Also, Fig. 1 shows that the carbon support is responsible for the broad reflection (002) observed in  $2\theta = 25^\circ$ . This effect is easily observed in diffractograms (c) and (d). The relative intensity of this broad reflection decreases with the increase of Pt in the samples due to the high intensity of Pt diffraction intensities with respect to the carbon signal. All other reflection peaks not related to Pt and C are related to a

mixture of  $\text{PbO}_x$  crystallites (mixtures of  $\text{PbO}$  and  $\text{PbO}_2$ ) as characterised in previous work from our group [21]. Therefore, as discussed in these previous publications, all catalysts are formed by unalloyed, separated Pt and  $\text{PbO}_x$  crystallites.

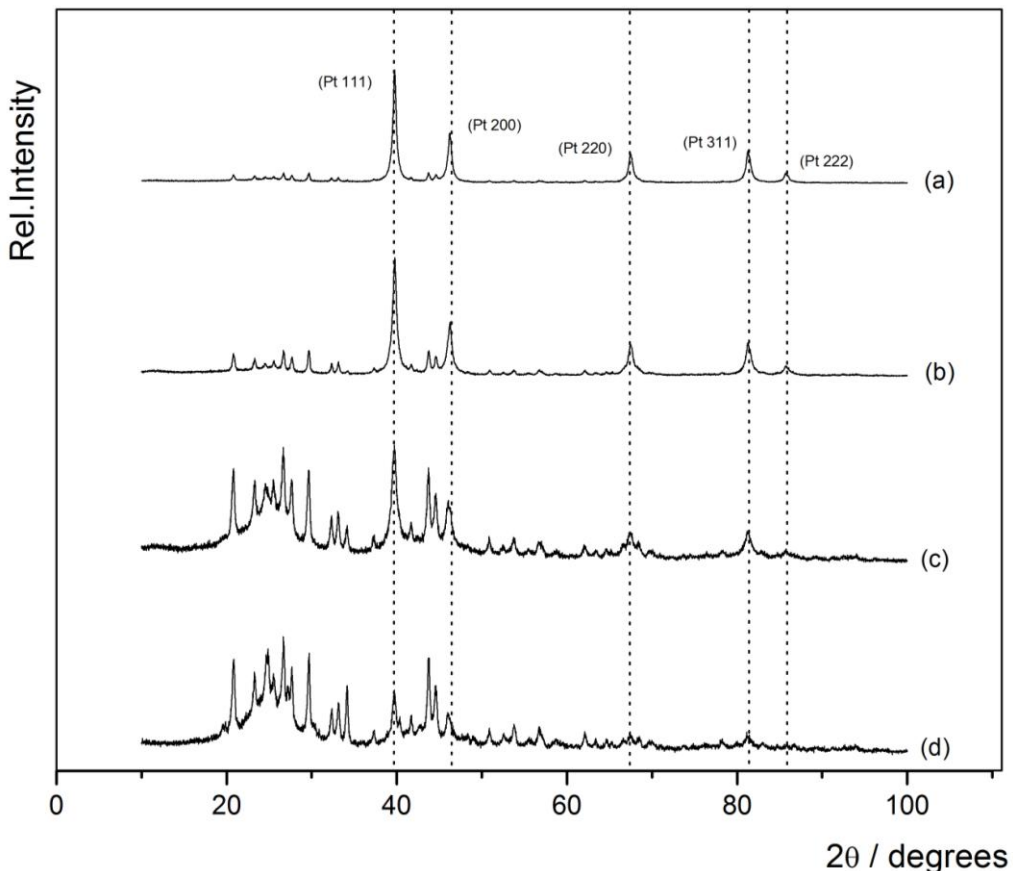


**Figure 1.** X-ray diffraction patterns of Pt and Pb-based catalysts with a fixed catalyst load of 10% with respect to the carbon powder support for (a) 90% Pt - 10% Pb, (b) 75% Pt - 25% Pb, (c) 25% Pt - 75% Pb and (d) 10% Pt - 90% Pb.

TEM images were obtained to determine the catalysts' particle sizes and spatial distributions for the 10% metal load materials. Fig. 2 shows representative images for two selected systems (90% Pt - 10% Pb and 10% Pt - 90% Pb) and respective mean particle diameter distribution.

The particles of both systems have a general spheroidal shape and a sharp size distribution with mean particle sizes of  $4.8 \text{ nm} \pm 3.7 \text{ nm}$  for the 90% Pt - 10% Pb catalyst and  $2.5 \text{ nm} \pm 1.8 \text{ nm}$  for the 10% Pt - 90% Pb catalyst. The particles of both systems appear spatially dispersed on the support, but a significant population of particle aggregates as well as bare support areas were observed. The morphological heterogeneity of a 50% Pt - 50% Pb material was already demonstrated in an extensive analytical electron microscopy study published by our group [20]. The majority of the particles were described as metallic Pt particles that are surrounded by very small particles and atomic clusters of  $\text{PbO}_x$ . These  $\text{PbO}_x$  entities are homogeneously distributed on the carbon support. This homogeneous distribution of lead oxide explains the good performance of this kind of catalyst despite the occurrence

of some degree of Pt particle aggregation because each Pt particle deposited on the carbon grain will have a lead oxide cluster or particle beside it.

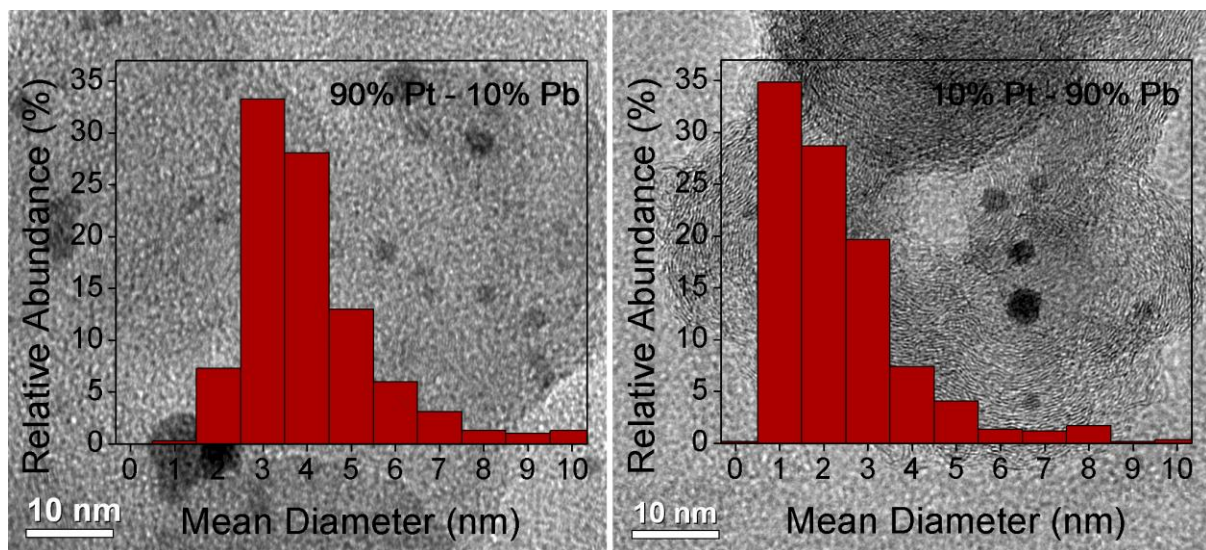


**Figure 2.** TEM images for two selected Pt and Pb-based catalysts: 90% Pt - 10% Pb and 10% Pt - 90% Pb and respective histograms of mean particle diameter distribution. Despite the measured sharp size distribution, particle aggregation was observed in both catalysts.

After physical characterisation, electrochemical tests were carried out for all synthesised electrodes. The total geometric area and quantity of ink deposited onto the glassy carbon electrode were kept constant for all experiments. Currents are presented in terms of absolute currents ( $I$ ). The normalisation of currents could result in inconsistent data in this study because this discussion is based on the comparison of each electrochemical response.

Cyclic voltammograms presented in Fig. 3 show a comparison of all studied materials with a fixed catalyst load of 10% with respect to the carbon powder content. It is interesting to observe the effect of lead in the materials. As seen in Fig. (3-a), the 100% Pt catalyst exhibits a classical behaviour for the metallic polycrystalline Pt with very low currents of oxidation of formic acid in the direct scan and a very high current of oxidation in the reverse scan. These reaction mechanisms were discussed in a previous paper published by our group [21]. This behaviour is related to the indirect mechanism of oxidation of formic acid in Pt, which involves the chemical adsorption of CO followed by 2 electrochemical steps (1 electron per step) [22].. When lead is added in a proportion of 10% (see Fig. 3-b) with respect to the platinum, the behaviour is quite similar to that presented in Fig. (3-a). On the other hand, the role of lead starts to appear in the catalyst composed by 75% Pt – 25% Pb, as can be seen in Fig. (3-c). In this figure, the peak currents of oxidation are about 12 times higher than those observed for the material composed of 90% Pt – 10% Pb. Figs. 3-d, 3-e and 3-f show the effective role of lead in this kind of catalyst: the behaviour demonstrated by these curves is quite different from what has been previously reported. For these kinds of catalysts, the oxidation occurs preferentially by the direct pathway when HCOOH is directly oxidised to  $\text{CO}_2$  in a reaction involving two electrons in one

single step [21]. All of these materials present high currents of oxidation and begin the electrochemical process in very low potentials (about 0.2 V vs. HESS).

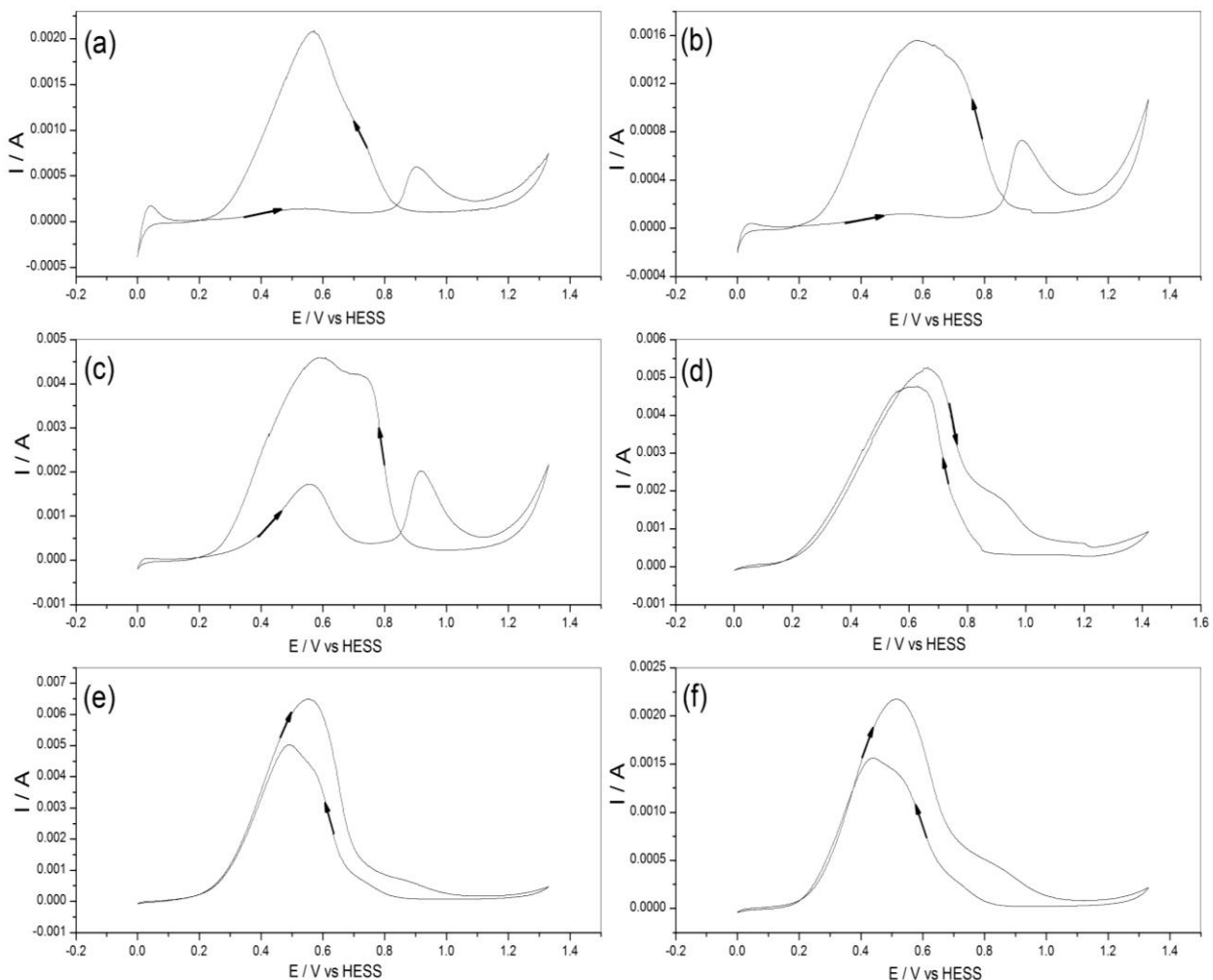


**Figure 3.** Cyclic voltammetry carried out in a solution of  $0.5 \text{ mol L}^{-1} \text{H}_2\text{SO}_4 + 1.0 \text{ mol L}^{-1} \text{HCOOH}$  for the Pt and Pb-based catalysts with a fixed catalyst load of 10% for the following catalysts: (a) 100% Pt, (b) 90% Pt - 10% Pb, (c) 75% Pt - 25% Pb, (d) 50% Pt - 50% Pb, (e) 25% Pt - 75% Pb and (f) 10% Pt - 90% Pb. Scan rate =  $20 \text{ mVs}^{-1}$ .

In a comparison of the three voltammogram curves, the catalyst composed of 25% Pt – 75% Pb presented the highest current values during the direct scan.

Corroborating with the cyclic voltammetries, Short-time chronoamperometric studies, which are presented in Fig. 4, corroborate the cyclic voltammetry results and demonstrate that the catalyst composed of 25% Pt – 75% Pb presented the highest current values during the operation time.

For this composition, a considerable quantity of bubbles was observed during the experiment and the observed noise (pink curve, 25% Pt – 75% Pb catalyst) is related to this fact. Formic acid oxidation for the 100% Pt and 90% Pt – 10% Pb electrodes presented negligent oxidation currents for

this fixed potential of operation of 0.3 V vs. HESS. The synergistic effects of lead in the catalysts can also be observed in this figure.

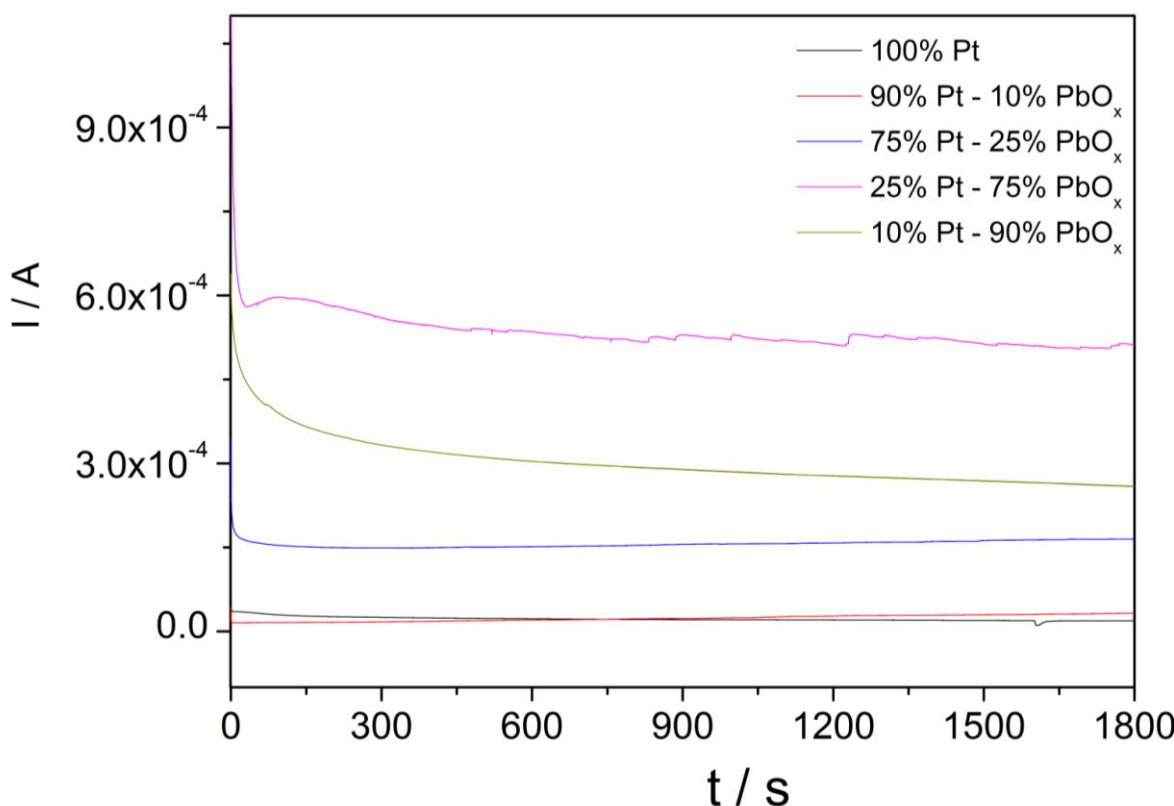


**Figure 4.** Short-time electrochemical responses for several catalysts with a fixed catalyst load of 10 % with respect to the carbon powder support carried out in a solution of  $0.5 \text{ mol L}^{-1} \text{H}_2\text{SO}_4 + 1.0 \text{ mol L}^{-1} \text{HCOOH}$ . Time of operation = 1800 s. The experiment was carried out at a fixed potential of 0.3 V vs. HESS.

#### 4. CONCLUSION

As expected, DRX characterisation demonstrated that a higher Pt quantity is related to a higher polycrystalline platinum signal, which qualitatively demonstrates that the synthesis was well done. Also, it was determined that the electrode was composed of separated phases of Pt and lead, and alloy formation was not observed. These catalysts are composed primarily of nanometric-sized islands that are heterogeneously dispersed onto the carbon as shown in the TEM images. In addition, electrochemical tests (cyclic voltammetry and short-time chronoamperometries) indicate that out of all the studied catalysts, the 25% Pt – 75% Pb material performed best.

#### ACKNOWLEDGEMENTS

We thank the Brazilian agencies FAPESP (2007/05155-1, 2007/05370-0), CNPq (472476/2008-4, 301863/2008-3 and 483452/2010-6), CAPES, UFABC and LME-LNLS (JEOL JEM 2100 TEM-MSC)

## References

1. C. Rice, S. Ha, R.I. Masel, A. Wieckowski, *J. Power Sources*, 115(2003)229.
2. C. Rice, S. Ha, R.I. Masel, P.Waszczuk, A.Wieckowski, *J. Power Sources*, 111(2002)83.
3. Y. Zhu, Z. Khan, R.I. Masel, *J. Power Sources*, 139(2005)15.
4. S. Ha, R. Larsen, Y. Zhu, R.I. Masel, *Fuel Cells*, 4(2004)337.
5. X.W. Yu, P.G. Pickup, *J. Power Sources*, 192(2009)279.
6. E. Casado-Rivera, D.J. Volpe, L. Alden, C. Lind, C. Downie, A.C.D. Angelo, F. J. DiSalvo, H.D. Abruña, *J. Am. Chem. Soc.*, 126(2004)4043.
7. R.V. Niquirilo, E. Teixeira-Neto, G.S. Buzzo, H.B. Suffredini, *Int. J. Electrochem. Sci.*, 5(2010)344.
8. C. Roychowdhury, F. Matsumoto, V.B. Zeldovich, S.C. Warren, P.F. Mutolo, M. Ballesteros, U. Wiesner, H.D. Abruña, F.J DiSalvo, *Chem. Mater.* 18(2006)3365.
9. S. Patra, H. Yang, H., *Bull. Korean Chem. Soc.* 30(2009)1485.
10. H. B. Suffredini, G. R. Salazar-Banda, L. A. Avaca, *J. Power Sources* 171(2007)355.
11. A.J. Terezo and E.C. Pereira, *Materials Letters*, 53(2002)339.
12. L.G. Bulusheva, A.V. Okotrub, A.G. Kurenya, H. Zhang, H. Zhang, X. Chen, H. Song, *Carbon*, 49(2011)4013.
13. G.R Salazar-Banda, H.B. Suffredini, L.A. Avaca, *J. Braz. Chem Soc.*, 16(2005)903.
14. R. Lin, C. Cao, H. Zhang, H. Huang, J. Ma, *Int. J. Hydrogen Energy*, (2011) in press.
15. W. Li, Q. Xin, Y. Yan, *Int. J. Hydrogen Energy*, 35(2010)2530.
16. G.A. Camara, R.B de Lima, T. Iwasita, *Electrochem. Comm.* 6(2004)812.
17. H.A. Gasteiger, S.S. Kocha, B. Sompalli, F.T.Wagner, App. Cat. B – Enviromental, 56(2005)9.
18. K. Sasaki, J.X. Wang, M. Balasubramanian, J. McBreena, F. Uribe, R.R. Adzic, *Electrochim. Acta*, 49(2004)3873.
19. E. Billy, F. Maillard, A. Morin, L. Guetaz, F. Emieux, C. Thurier, P. Doppelt, S. Donet, S. Mailley, *J. Power Sources*, 195(2010)2737.
20. E. Teixeira-Neto, G.S. Buzzo, H.B. Suffredini, *J. Phys. Chem C*, 114(2010)9227.
21. G.S. Buzzo, R.V. Niquirilo, H.B. Suffredini, *J. Braz. Chem. Soc.* 21(2010)185.
22. A.Mikołajczuk, A. Borodzinski, P. Kedzierzawski, L. Stobinski, B. Mierzwa, R. Dziura, *App. Surf. Sci.*, 257(2011)8211.